

# Lipid-protein interaction induced domains: kinetics and conformational changes in multicomponent vesicles

K. K. Sreeja<sup>1, a)</sup> and P. B. Sunil Kumar<sup>2, b)</sup>

<sup>1)</sup>*Department of Physics, Indian Institute of Technology Madras, Chennai 600036, India, Department of Chemical and Bio-molecular Engineering, University of Pennsylvania, Philadelphia, PA 19104, USA.*

<sup>2)</sup>*Department of Physics, Indian Institute of Technology Madras, Chennai 600036, India, Department of Physics, Indian Institute of Technology Palakkad, Palakkad, 678557, India.*

(Dated: March 15, 2022)

The spatio-temporal organization of proteins and the associated morphological changes in membranes are of importance in cell signaling. Several mechanisms that promote the aggregation of proteins at low cell surface concentrations have been investigated in the past. We show, using Monte Carlo simulations, that the affinity of proteins for specific lipids can hasten its aggregation kinetics. The lipid membrane is modeled as a dynamically triangulated surface with the proteins defined as in-plane fields at the vertices. We show that, even at low protein concentrations, strong lipid-protein interactions can result in large protein clusters indicating a route to lipid mediated signal amplification. At high protein concentrations the domains form buds similar to that seen in lipid-lipid interaction induced phase separation. Protein interaction induced domain budding is suppressed when proteins act as anisotropic inclusions and exhibit nematic orientational order. The kinetics of protein clustering and resulting conformational changes are shown to be significantly different for the isotropic and anisotropic curvature inducing proteins.

Keywords: membrane remodeling, domain formation, lipid-protein interaction, monte carlo simulations

---

<sup>a)</sup>Electronic mail: [sreeja@seas.upenn.edu](mailto:sreeja@seas.upenn.edu)

<sup>b)</sup>Electronic mail: [sunil@iitm.ac.in](mailto:sunil@iitm.ac.in)

# I. INTRODUCTION

Protein redistribution and clustering on the cell surface are important for signal transduction pathways<sup>1</sup>. At its low physiologically relevant cell surface concentrations, direct interaction between proteins cannot be the primary cause for clustering, and many active and passive mechanisms, that indirectly aid protein clustering have been proposed<sup>2-5</sup>. The specialized membrane domains known as rafts, which is the result of a sterol and sphingolipid enriched aggregation, are believed to be one of the precursors for the protein clustering process<sup>1,6,7</sup>. Such membrane domains are often associated with peripheral and integral proteins<sup>8-13</sup>. Rafts are known to make a suitable platform for aggregation of GPI(glycosylphosphatidylinositol)- anchored proteins, which correspond to a set of exoplasmic, eukaryotic proteins exhibiting specific intracellular sorting and signaling properties<sup>5,14</sup>. Caveolin and clathrin are some of the non raft proteins associated with lipid domains<sup>2,15,16</sup>. Caveolae are glycolipid enriched domains, that are flask like invaginations formed by the assembly of Caveolin proteins. It is not clear if these lipid-protein domains arise from the direct interactions between the proteins or due to the interaction between non-protein membrane constituents and the affinity of proteins to certain membrane composition<sup>17,18</sup>.

Another factor that has lead to considerable interest in understanding the mechanisms behind lipid-protein sorting in biological membranes is the asymmetric distribution of lipids and proteins in the intercellular organelles such as the golgi and endoplasmic reticulum<sup>19,20</sup>. Lipids can dynamically vary the constituents of a membrane by selectively recruiting various proteins which in turn can change the functionality of the membrane, and similarly proteins can sort lipids to specific membrane locations through steric or electrostatic interactions<sup>21-23</sup>.

The membrane protein aggregation due to lipid-protein interactions has been studied using coarse grained molecular dynamics approaches when the length scale of interest are of few tens of nanometers<sup>23</sup>. Since our aim here is to explore the role of lipid-protein interaction in the formation of domains and since the length scale of the resulting conformational changes are much larger than the membrane thickness, we consider a mesoscale computational approach. Existing computational studies on the equilibrium or dynamic properties of membranes mostly deals with lipid phase separation following a quench into the two phase coexistence regime<sup>24-27</sup>. Experimental validation of the results from mesoscale simulations<sup>28</sup> has motivated further studies on the dynamics of these domains<sup>29</sup>. However,

there are very few attempts to understand how the interaction of proteins with other membrane constituents can lead to compositional inhomogeneities and clustering of proteins. Here we use a Monte Carlo model for a three component fluid vesicle, with one component representing protein inclusions and the others two different compositions of lipids, to investigate how lipid-protein interactions affect the kinetics of domain formation and associated conformational changes in the vesicle. To study protein clustering in detail, in our model, we also account for the direct protein-protein interactions and the membrane curvature inducing properties of the proteins.

The paper is organized as follows. In Section II, we describe the Monte Carlo model for a multi-component membrane. In the results and discussions given in Section III, we first focus on the lipid domain formation. A comparison of the kinetics of lipid-protein interaction induced domain formation with that due to lipid-lipid interaction is presented in Section III A. Conformational changes of the membrane for different protein concentrations are also discussed here. In Section III A 1, we present results on the effect of combined lipid-lipid and lipid-protein interaction on domain growth. In the second part of Section III, we present our results on protein cluster growth with varying lipid and protein concentrations. Section III B 2 and III B 3 is dedicated, respectively, to discussion on how explicit protein-protein interactions and the curvature remodeling activity of proteins affect cluster growth.

Our main results are the following. We show that the affinity of proteins for certain type of lipids can lead to formation of large protein clusters even at low concentration of proteins. The increase in protein cluster growth rate, due to strong lipid-protein interaction, indicate a route to lipid mediated signal amplification. It is pointed out that the absence of line tension at the domain boundary, at low protein concentration, is the primary reason for enhanced kinetics of domain growth. The domain growth is slower at high protein concentrations and when proteins act as anisotropic inclusions to exhibit nematic orientational order.

## II. MODEL

In the Monte Carlo simulations carried out here, the conformation of a lipid membrane is approximated to be that of an elastic sheet represented by a randomly triangulated surface. In this scheme, a vesicle of spherical topology is represented by  $N_v$  vertices,  $N_L = 3(N_v - 2)$  links and  $N_T = 2(N_v - 2)$  triangles and the triangulation is changed randomly to simulate

the in-plane fluidity of the membrane. In the case of an isotropic and homogeneous membrane, the energetics of the elastic sheet is described using a discretized form of the Helfrich Hamiltonian,

$$\mathbf{H}_{\text{elastic}} = \frac{\kappa}{2} \sum_{v=1}^{N_v} (2H_v - C_0)^2 A_v, \quad (1)$$

where summation is over all the vertices of the triangulated membrane. Here  $\kappa$  is the bending rigidity of the membrane,  $C_0$  is the spontaneous curvature resulting from lipid asymmetry of protein induced deformations in the bilayer,  $H_v$  is the mean curvature defined at the vertex and  $A_v$  is the area associated with the vertex  $v$ , computed as in Ramakrishnan et. al.<sup>30</sup>.

To model a multicomponent vesicle with two coexisting lipid compositions and one type of protein, we introduce a lipid composition field  $\phi_v$  and a protein field  $p_v = 1$ , both positioned on the membrane vertices. The lipid field  $\phi_v = 1$  when the composition of lipid at vertex  $v$  is labelled A and  $\phi_v = -1$  if the lipid composition is labelled B. Similarly  $p_v = 1$  in the presence of a protein at the vertex and  $p_v = 0$  otherwise. A vertex can be simultaneously occupied both by the protein and the lipid fields. Lipid-lipid interactions are assumed to be Ising like. The two component lipid vesicle model has been previously used to study the lipid induced phase separations and budding of domains<sup>25</sup>. The Hamiltonian describing explicit lipid-lipid interactions is given as

$$\mathbf{H}_\phi = -J_\phi \sum_{\langle vv' \rangle} \phi_v \phi_{v'}, \quad (2)$$

where the summation runs over all the neighboring pairs.

The lipid-protein interaction is modeled using the Hamiltonian,

$$\mathbf{H}_{p\phi} = -J_{p\phi} \sum_{\langle vv' \rangle'} p_v \phi_{v'}. \quad (3)$$

The prime on the summation indicates that the protein field at any vertex is allowed to interact with the lipids within the one ring neighborhood including its own vertex. When we choose  $J_{p\phi} > 0$ , the lipid-protein interaction is attractive between the proteins and type A lipids. Since A lipids are miscible in B lipids and is the minority component, in this article we will often refer to lipid composition of type A as co-lipid.

The presence of curvature active proteins modulate local membrane shapes by inducing spontaneous curvature. We study two classes of curvature generating proteins: the first kind of proteins induce a uniform mean curvature on the membrane and the second kind

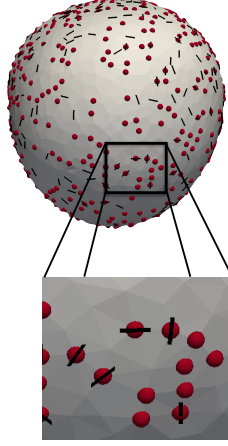


Figure 1. An illustration of a multicomponent vesicle: type A lipids are marked as spheres while the unmarked vertices correspond to type B lipids. The protein inclusions are shown by black lines.

are structurally anisotropic proteins, inducing directional curvatures. To model an isotropic curvature generating protein we consider the spontaneous curvature  $C_0$  (see Eqn.1) at any vertex to be nonzero in presence of a protein. The second class of proteins or protein complexes have an extended structure and cannot be considered as point like objects<sup>31</sup>. To incorporate the structural anisotropy of such a protein into the model we introduce a unit orientation vector  $\hat{\mathbf{n}}_v$  such that the in-plane protein field is now a vector  $\mathbf{p}_v = p_v \hat{\mathbf{n}}_v$ . The anisotropic shape of the protein is reflected by the rotational asymmetry of  $\hat{\mathbf{n}}_v$ . In this paper we consider only the case wherein  $\hat{\mathbf{n}}_v$  has a  $\pi$  rotational symmetry representing elongated protein inclusions<sup>30</sup>. The protein field thus acts like a nematic orientational field on the membrane. The explicit orientational interaction between the proteins on the membrane is modeled using the Lebwohl-Lasher model<sup>32</sup>, given by

$$\mathbf{H}_{LL} = -\epsilon_{LL} \sum_{\langle vv' \rangle} p_v p_{v'} \left\{ \frac{3}{2} \cos^2 \Phi(\hat{\mathbf{n}}_v, \hat{\mathbf{n}}_{v'}) - \frac{1}{2} \right\}, \quad (4)$$

where,  $\Phi(\hat{\mathbf{n}}_v, \hat{\mathbf{n}}_{v'})$ , the angle between the two in-plane field vectors on the tangent planes at neighboring vertices  $v$  and  $v'$ , is computed using a parallel transport operation<sup>30</sup>. The protein orientation field is coupled to the membrane curvature using a discretized version of the Hamiltonian proposed by Frank and Kardar<sup>33</sup>,

$$\mathbf{H}_{\text{anis}} = \sum_v \left[ \frac{\kappa_{\parallel}}{2} (H_{n,\parallel} - C_0^{\parallel})^2 + \frac{\kappa_{\perp}}{2} (H_{n,\perp} - C_0^{\perp})^2 \right] A_v. \quad (5)$$

$H_{n,\parallel}$  and  $H_{n,\perp}$  are the curvatures along the directions  $\hat{\mathbf{n}}_v$  and  $\hat{\mathbf{n}}_v^{\perp}$  respectively.  $C_0^{\parallel}$  and  $C_0^{\perp}$

are the local directional spontaneous curvatures and  $\kappa_{\parallel}$  and  $\kappa_{\perp}$  are the bending stiffness along  $\hat{\mathbf{n}}_v$  and  $\hat{\mathbf{n}}_v^{\perp}$ , respectively. The anisotropic protein inclusions considered in our study generate additional stiffness and curvatures only along the direction  $\hat{\mathbf{n}}$ , i.e., we consider only the cases with  $\kappa_{\perp} = 0$ .

The multicomponent vesicle is equilibrated through a set of Monte Carlo (MC) moves with the total effective Hamiltonian:

$$\mathbf{H}_{\text{total}} = \mathbf{H}_{\text{elastic}} + \mathbf{H}_{p\phi} + \mathbf{H}_{\phi} + \mathbf{H}_{\text{anis}} + \mathbf{H}_{LL}. \quad (6)$$

We only consider the case of conserved in-plane fields and the MC moves include the vertex moves, link flips,  $\mathbf{p}$  field rotations and the exchange of  $\mathbf{p}$  and  $\phi$  fields <sup>30,34</sup>. Unless otherwise stated, all moves are accepted through the Metropolis algorithm. (a) *Vertex move*: Here the position of a vertex is updated to a new position chosen randomly within a cutoff distance. This cutoff is fixed such that 50% of the moves are accepted. This move allows for shape changes of the vesicle. (b) *Link flip*: A randomly selected edge, connecting two triangles, is disconnected and a new connection between the unconnected vertices of the same triangles is constructed. This move changes the triangulation/connectivity and physically models the fluidity of the bilayer membrane by allowing the vertices to diffuse through the surface. (c) *Exchange of  $\phi$  fields*: The diffusion of lipid composition field on the membrane surface is captured using a Kawasaki move that allows for an exchange between type A and type B vertices. (d) *Exchange of  $\mathbf{p}$  fields*: The diffusion of protein field on the membrane surface is captured using a Kawasaki exchange move. (e)  *$\mathbf{p}$  field rotation*: In this step, a vertex is chosen randomly and the orientation field at the chosen vertex, if nonzero, is rotated to a new, randomly chosen direction in the tangent plane. This rotation of the field allows for the relaxation of the orientational order of the field.

The multicomponent membrane system described here is studied using vesicles with 2030 vertices and 4056 triangles. We consider a vesicle with bending rigidity  $\kappa = 10 k_B T$ . Initial configurations of the vesicle are generated by randomly assigning  $\phi\%$  of the membrane vertices to have lipids of type A and the rest of the vertices are assigned to have type B lipids. The proteins, whose number fraction is represented by  $p\%$ , are also placed at randomly chosen vertices with random in-plane orientations. A patch of the membrane with co-existing lipid and protein fields is shown in Fig. 1 and we follow the same representation for further discussions. It should be noted that even when the proteins are not anisotropic in

nature they are represented by solid black lines in order to distinguish them from lipid-type specification on the vertices.

### III. RESULTS AND DISCUSSIONS

#### A. Lipid clustering due to protein-lipid interaction

To investigate membrane inhomogeneities induced by the lipid-protein interactions, we first consider the case of isotropic inclusions, such that  $\mathbf{H}_{\text{anis}}$  and  $\mathbf{H}_{LL} = 0$ , no direct lipid-lipid interactions (i.e.  $\mathbf{H}_\phi = 0$ ) and focus on the aggregation kinetics that is solely driven by lipid-protein interaction  $\mathbf{J}_{p\phi} > 0$ . For these parameters, the proteins only serve to promote the aggregation of lipids and do not have any direct impact on local membrane shapes. In our model the lipids and proteins can occupy the same vertex and lipid-protein interaction is limited to nearest neighbor sites. The relative values of  $\phi\%$  and  $p\%$  is thus another important parameter. Below we first analyze the cluster growth when  $p\% < \phi\%$ .

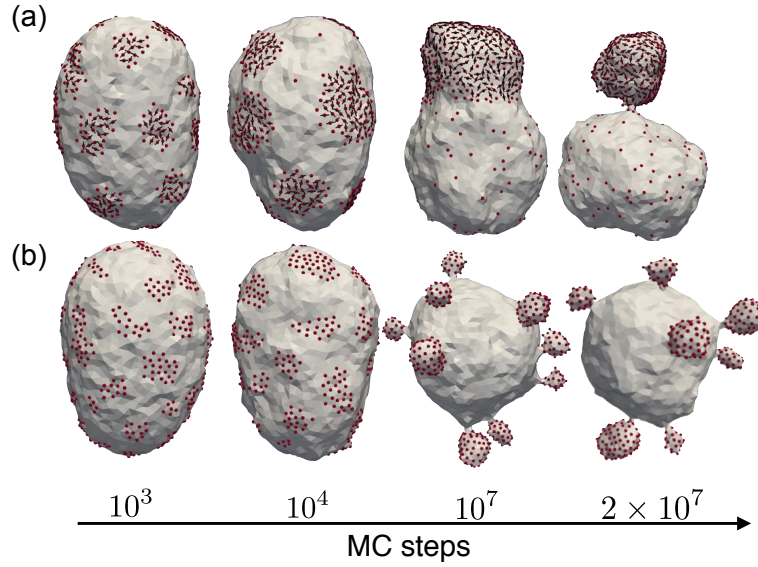


Figure 2. A comparison of domain formation with  $p - \phi$  and  $\phi - \phi$  interactions as a function of MC steps. (a) Conformations of a vesicle when lipids aggregate through  $p - \phi$  interactions for  $J_\phi = 0$ ,  $J_{p\phi} = 2$ ,  $\phi\% = 30$  and  $p\% = 20$ . (b) Lipid clusters induced by  $\phi - \phi$  interactions for  $J_\phi = 2$ ,  $\phi\% = 30$  and  $p\% = 0$ .

*Clustering kinetics:* The evolution of membrane inhomogeneities and the associated vesicle conformations, as a function of MC time, are shown in Fig. 2. Panel (a) shows  $p - \phi$  interaction driven clustering when  $\mathbf{H}_{p\phi} > 0$ ,  $\mathbf{H}_\phi = 0$ ,  $\phi\% = 30$  and  $p\% = 20$ . For comparison panel (b) shows membrane conformations for lipid-lipid interaction induced aggregation, when  $\mathbf{H}_{p\phi} = 0$ ,  $\mathbf{H}_\phi > 0$ ,  $\phi\% = 30$  and  $p\% = 0$ . As can be inferred from the figure, the kinetics of clustering and conformational changes in the membrane are significantly different in these two cases. The evolution of vesicle shape, resulting from direct lipid-lipid interactions, shown in panel (b) of Fig. 2, is similar to that observed in previous studies<sup>25</sup>. At early times (MC steps  $\leq 10^4$ ), in both cases, domains of co-lipids nucleate and grow into stable clusters as shown in Fig. 2. As can be seen in panel (a),  $p - \phi$  interaction is sufficient to induce an effective attraction between the lipids and trigger the formation of co-lipid patches. The late time growth of domains, however, is strongly dependent on the nature of interactions. When  $\phi\% > p\%$ , in the case of protein induced segregation, shown in panel (a), the domains remain flat and their aggregation is fast. While in panel (b), the presence of explicit lipid-lipid interaction leads to budding and slowing down of coarsening.

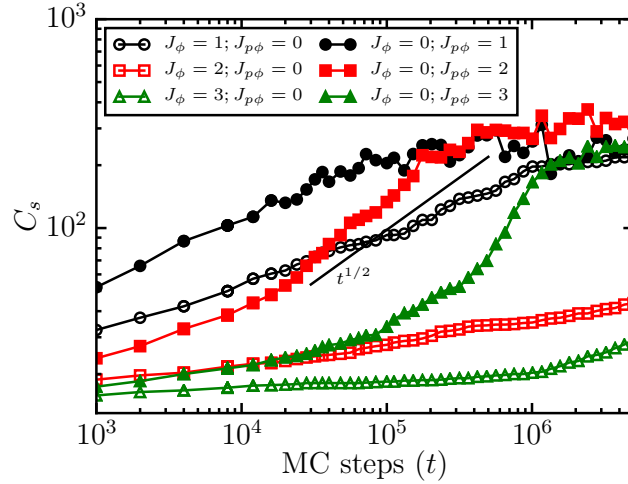


Figure 3. Comparison of lipid cluster growth with  $p - \phi$  and  $\phi - \phi$  interactions when  $\phi\% = 30$ . Average cluster size of type A domains for different values of  $J_\phi$  and  $J_{p\phi}$  is given. When  $J_\phi = 0$  (filled symbols) protein concentration is fixed at  $p\% = 20$  while for  $J_\phi > 0$  (open symbols), it is taken to be  $p\% = 0$ .

A quantitative comparison of domain growth can be obtained by analyzing the average



lipid cluster size as a function of time. The average cluster size for different values of the interaction strengths  $J_\phi$  and  $J_{p\phi}$  are given in Fig. 3. The cluster sizes ( $C_s$ ) correspond to the number of vertices of type A that form a continuous map on the triangulated surface. The early time domain growth is similar in all cases. When the coarsening is only through lipid-lipid interaction strength (i.e., for  $J_\phi > 0$  and  $J_{p\phi} = 0$ ), for all values of  $J_\phi$ , and for the system sizes considered here, the growth rate remains low and the system does not enter into a scaling regime. The coarsening is considerably faster with lipid-protein interaction  $J_{p\phi} > 0$  and we see a power law regime with  $C_s \propto t^{1/2}$ , which could result from domain diffusion and coalescence (see Appendix A), as the diffusion coefficient of domains, in the Rouse dynamics, varies as the inverse of the domain size (data not shown). The corresponding configurations are shown in Fig. 4. It is important to note that, for  $J_{p\phi} \leq 3$ ,  $J_\phi = 0$  and with  $\phi\% > p\%$ , the domains remain flat. This is evident from the  $Ls \propto t^{1/4}$  dependence of interfacial length  $Ls$  on time as shown in Fig. 5. On the other hand, in the case of clustering induced by direct lipid-lipid interactions, when the value of  $J_\phi$  is higher, the line tension is usually significant enough to induce budding. This regime can be easily identified in Fig. 5 as one with sudden fast decrease of interface length. The movement of domains, which now involve membrane shape changes, significantly slows down domain coarsening.

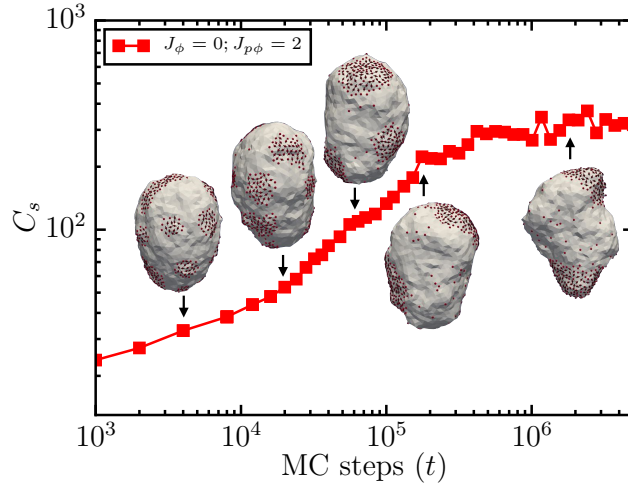


Figure 4. Coalescence of protein rich domains on the vesicle surface due to  $p - \phi$  interactions. The cluster sizes shown are for  $\phi\% = 30$ ,  $p\% = 20$ ,  $J_{p\phi} = 2$  and  $J_\phi = 0$ .

It is clear from the above discussions that the ability of domains to remain flat is important for fast clustering of proteins. In the model, positive values of  $J_{p\phi}$  favor type A lipids to

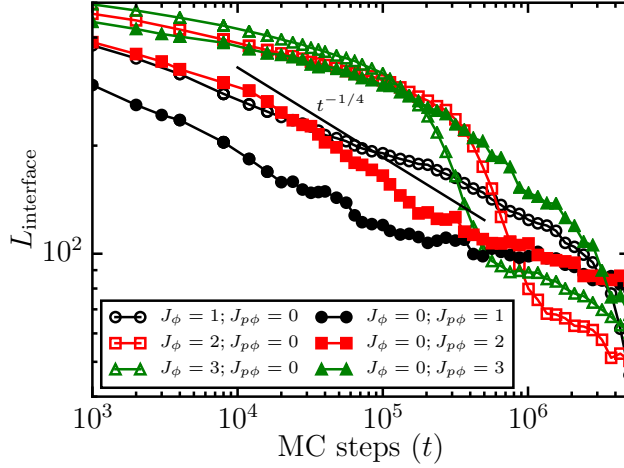


Figure 5. Comparison of lipid domain interfacial length for  $\phi - \phi$  and  $p - \phi$  interactions for various values of  $J_\phi$  and  $J_{p\phi}$  when  $\phi\% = 30$ . When  $J_\phi = 0$  protein concentration  $p\% = 20$  and  $L_{\text{interface}}$  is computed as the number of vertices occupied by the A lipids with atleast one type B lipid vertex as a neighbor.

occupy a vertex with a protein on it or in the one ring neighborhood of it. When the fraction of vertices occupied by the protein is much smaller than that of A lipids ( $\phi\% > p\%$ ), there are enough A lipids to occupy the one ring neighborhood even when there are many small protein clusters. In this regime, when  $J_\phi = 0$ , co-lipids at the boundary of the domains will act as surfactants and we expect the interfacial tension at the lipid-protein domain boundaries to be negligible resulting in flat domains. Such a surfactant lined domain could stabilize small clusters and prevent coarsening. But our simulations show a complete coalescence of domains, indicating that the entropy gain from release of excess co-lipids is significant enough to drive domain coarsening. Thus the protein induced domains show faster coalescence compared to the domains formed by direct lipid-lipid interaction.

*Conformational changes:* When  $J_\phi = 0$ , there are two main factors that affect the conformational changes of the membrane; (i) the fraction of vertices occupied by the proteins ( $p\%$ ) in comparison to that occupied by co-lipids ( $\phi\%$ ) and (ii) the interaction strength  $J_{p\phi}$ . Fig. 6 shows the representative equilibrium conformations for different values of  $p\%$  and  $J_{p\phi}$  for a fixed value of  $\phi\% = 30$ . When  $p\% = 10$ , large clusters are formed, but these clusters do not initiate budding even for large value of  $J_{p\phi}$ . As described in the previous section,

this is due to the presence of additional type A vertices at the interface that shields the protein from type B vertices and reduces the line tension. The domains start to deform when  $p\% = 20$  and  $J_{p\phi} = 2$ . At  $p\% = 30$  the number of proteins become equal to the number of type A vertices, and there are no additional co-lipids to line the domain interface. In this case when the lipid-protein domain size reaches a certain value it starts to bud.

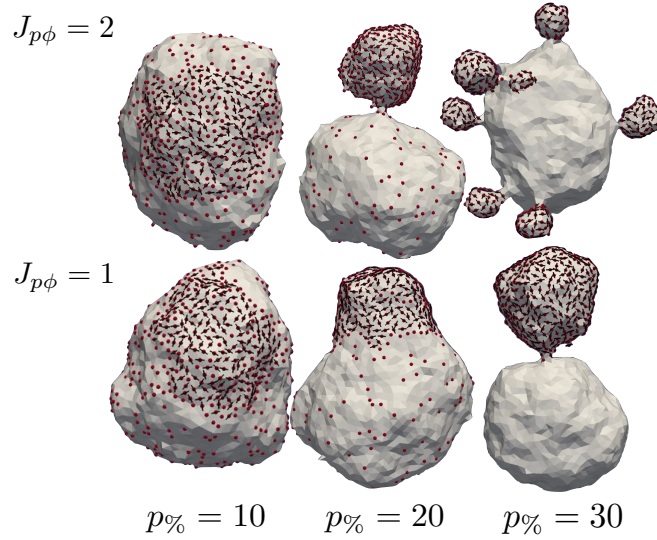


Figure 6. Phase separation and shape changes as a function of  $p\%$  and  $J_{p\phi}$  when  $\phi\% = 30$  and  $J_\phi = 0$ . Lipid domains starts to bud when  $p\% = 20$  and  $J_{p\phi} = 2$ . The snapshots are taken after  $2 \times 10^7$  MC steps.

### 1. *Effect of lipid-protein interaction at low co-lipid concentration*

In biological membranes both lipid-lipid and lipid-protein interactions are expected to affect the protein phase-segregation and hence a study of combined  $\mathbf{H}_\phi$  and  $\mathbf{H}_{p\phi}$  interactions are of relevance to cellular membranes. Here we study the effect of lipid-protein interactions by holding the lipid-lipid interaction fixed at  $J_\phi = 1$ . The average cluster size in this case when  $\phi\% = 30$  and  $p\% = 20$  is shown in Fig. 7. Here as  $J_{p\phi}$  increases the growth rate of lipid cluster size decreases in a monotonic fashion. When there is not enough co-lipids to cover all protein neighborhood and the protein domain boundary is occupied by both A and B lipids, non zero protein B lipid interaction, parameterized through  $J_{p\phi}$ , will increase the line tension at the boundary, resulting in domain shape changes. Such morphological changes

reduces domain diffusion and leads to a slow down in coalescence of domains and increases the life time of smaller domains.

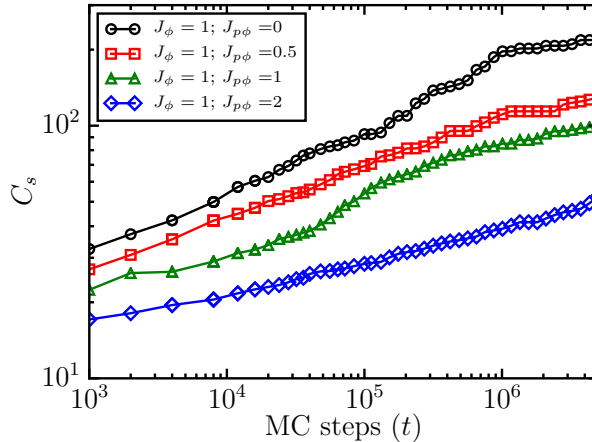


Figure 7. Average cluster size with lipid-protein and lipid-lipid interactions when  $\phi_{\%} = 30$  and  $p_{\%} = 20$  for  $J_{\phi} = 1$  and  $J_{p\phi} = 0, 0.5, 1$  and  $2$ .

## B. Protein clustering due to lipid-protein interaction

In this section we investigate how the lipid-protein interaction can change the effective protein clustering and the structural properties of protein inclusions affect protein clustering. In the following discussion we consider domain formation without explicit lipid-lipid interactions and constant lipid-protein interactions, i.e., we take  $J_{\phi} = 0$  and  $J_{p\phi} = 2$ .

### 1. Concentration of proteins and lipids

Here we study the aggregation of proteins at a smaller protein concentration compared to the previous cases. We keep  $p_{\%} = 10$  and study the domain formation by varying  $\phi_{\%}$ . The resulting conformations and the largest cluster sizes are shown in Fig. 8. As shown in panel(b), the domains bud for equal concentration of co-lipids and proteins. When  $\phi_{\%} > p_{\%}$  the line tension decreases and hence the domains remain flat. The increase in cluster sizes due to the flat domains can be seen in Fig. 8(a). When  $\phi_{\%} \geq 20$ , at early times we observe a domain growth that depends on the fraction of co-lipids present and at late times a complete

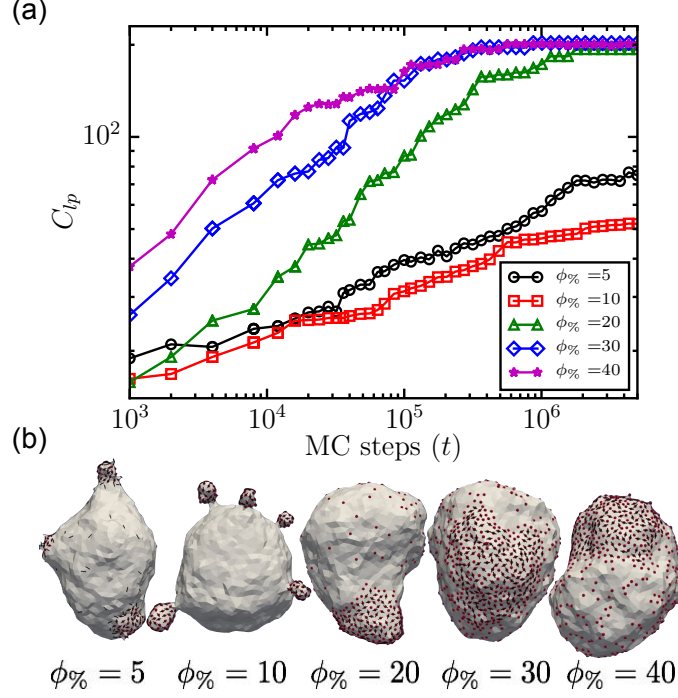


Figure 8. Protein aggregation at low protein concentration as a function of  $\phi_{\%}$  for  $p_{\%} = 10$ ,  $J_{\phi} = 0$  and  $J_{p\phi} = 2$ . Panel (a) shows the size of largest protein cluster as a function of time. Panel (b) shows representative vesicle conformations at MC steps =  $5 \times 10^6$ .

clustering of proteins. Even when  $\phi_{\%} \gg p_{\%}$  we observe a large cluster instead of small clusters. This could be due to the increase in entropy due to the configurational freedom of proteins in a larger cluster compared to small domains.

Complete protein clustering, even at low values of protein concentration and in the absence of any direct protein-protein interaction, can be achieved through lipid-protein interaction is one of the main results presented in this paper. To understand this more quantitatively we also looked at lipid-protein aggregation as a function of  $p_{\%}$  when  $\phi_{\%} = 30$ . In Fig. 9(a) we show  $C_{lp}/p_{\%}$  to represent the fraction of proteins clustered and in Fig. 9(b), the corresponding conformations at  $5 \times 10^6$  MC steps. For low protein concentrations ( $p_{\%} = 5, 10$ ) a complete clustering of proteins is observed. The fraction of protein clustered is minimum when  $p_{\%} = 30$ , which is equal to  $\phi_{\%}$ . This is expected as the line tension and membrane deformations are maximum when  $p_{\%} = \phi_{\%}$ .

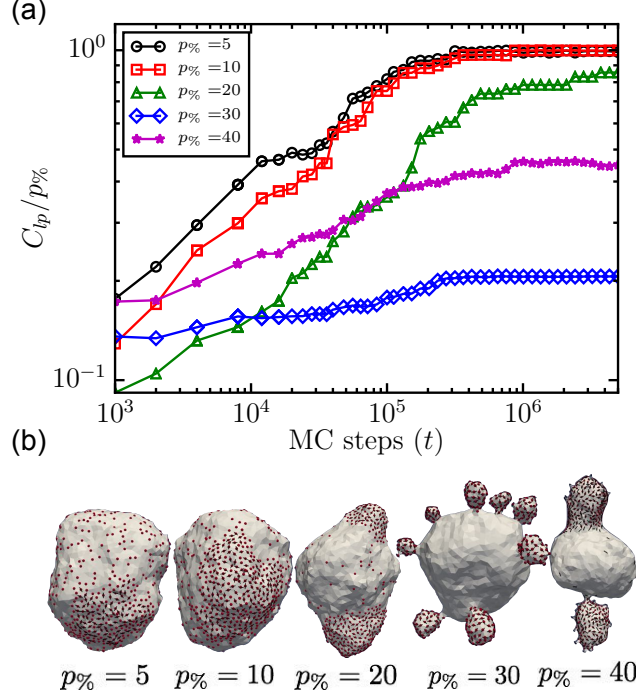


Figure 9. Protein clustering as a function of  $p\%$  when  $\phi\% = 30$ ,  $J_\phi = 0$  and  $J_{p\phi} = 2$ . Panel (a) shows  $C_{lp}/p\%$  as a function of time and (b) the vesicle conformations at  $MC \text{ steps} = 5 \times 10^6$ .

## 2. Explicit protein-protein orientational interactions

In this section we focus on the effect of a direct interaction between the proteins in addition to its interaction with lipids. Orientational interaction between proteins are relevant for elongated protein inclusions. The proteins are now treated as in-plane vector fields and their nematic like orientational interaction is modeled through the Lebwohl-Lasher energy functional<sup>35</sup>, which is given in Eqn. 4. This interaction is short ranged and is only between in-plane fields (proteins) within the connected neighborhood and captures the symmetry property of the nematic vectors. In an earlier study it has been shown that this orientational interaction ( $\mathbf{H}_{LL}$ ) alone can aggregate proteins on the surface and induce significant membrane conformational changes<sup>30</sup>.

In Fig. 10 we show the time evolution of protein domains on the vesicle with orientational order and fixed  $\mathbf{H}_{p\phi}$  interaction; panel (a) shows the largest protein cluster size and panel (b) the vesicle conformations as a function of time when  $\epsilon_{LL} = 3$ . We consider the case with  $p\% = 20$  and  $\phi\% = 30$ , to compare with the case discussed in Sec III A. From Fig. 10(a) it can be seen that as  $\epsilon_{LL}$  increases the cluster growth slows down. As  $\epsilon_{LL}$  increases the additional

attractive interaction between the components reduces the diffusivity of the protein cluster which in turn reduces the rate of growth of clusters. When  $\epsilon_{LL} = 0$  (see panel (a) of Fig. 2),  $\mathbf{H}_{p\phi}$  interaction induces domains that are nearly circular in shape which, at a later stage, coalesce and bud off. When  $\epsilon_{LL} > 0$  (see panel (b) of Fig. 10), domains with non-circular boundaries are formed first. Within a domain the protein fields are aligned in one direction. As time progress the domain boundaries take a circular shape. However, due to the energy cost in maintaining parallel orientation of the protein field, the domains do not bud as in the case with  $\epsilon_{LL} = 0$ .

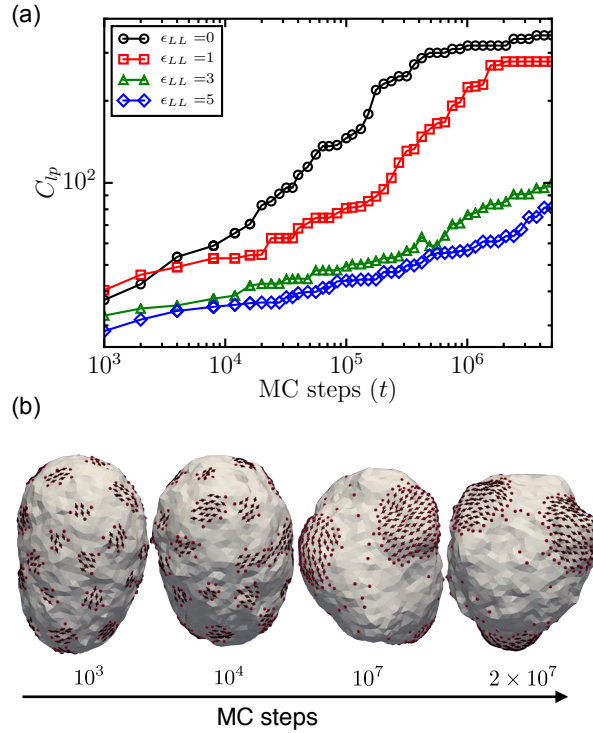


Figure 10. Formation of protein clusters with explicit protein-protein interaction when  $J_{p\phi} = 2$ ,  $J_\phi = 0$ ,  $p\% = 20$  and  $\phi\% = 30$ . Panel (a) is the largest protein cluster size and (b) the vesicle conformations when  $\epsilon_{LL} = 3$ .

### 3. Curvature active proteins

Collective interactions of curvature generating membrane associated proteins, like BAR domain proteins, caveolin and clathrin can lead to interesting shape transformations in organelle membranes. Protein induced lipid sorting has been shown with compelling evidences

in the trans-golgi and endosomal membranes and it is believed that sorting happens in response to the curvature induced by the proteins<sup>2,15,16,36</sup>. The presence of curvature inducing and curvature sensing proteins in lipid domains can significantly alter the composition of the domain since these proteins are known to have a strong affinity for certain class of lipids<sup>37–39</sup>. Here we discuss how the protein field induced curvature along with lipid-protein interactions, can alter the protein domain growth and the shape of the vesicle. The domain formation due to two different classes of proteins: isotropic and anisotropic curvature generating proteins, are considered.

*Aggregation due to isotropic curvature generating proteins:* The spontaneous curvature generated by proteins is accounted via Eqn. 1 by assigning  $C_0 > 0$  to the vertices occupied by the proteins. The clustering kinetics and the corresponding conformations when  $\phi\% = 30$ ,  $p\% = 20$  are shown in Fig. 11. As can be seen in Fig. 11(a), at early times (MC steps  $\leq 10^5$ ) the growth curve is nearly independent of the value of  $C_0$ . For MC steps  $\geq 10^5$  the protein cluster size saturates at a value that decreases with increasing  $C_0$ . The membrane deformations due to curvature active proteins are observed only when these proteins form a cluster. When the cluster size reaches a threshold, at a value which depend on  $C_0$ , membrane starts to deform and this is reflected in the diffusion and growth of the clusters. In Sec III B 1 we have seen bud formation, induced by line tension, takes place only when  $\phi\% \leq p\%$ . Here we show that such buds can be formed even when  $\phi\% > p\%$  if the proteins are curvature active. Earlier such effects, of spontaneous curvature on vesicle conformations, have been studied only with direct lipid-lipid interaction induced clustering<sup>25</sup>.

*Aggregation due to anisotropic curvature generating proteins:* In order to study the role of anisotropic curvature induction in protein clustering we introduce curvature effects through the anisotropic curvature Hamiltonian given in Eqn. 5. We concentrate on the conformations of the membrane when  $\phi\% = 30$ ,  $p\% = 20$  and  $\kappa_\perp = 0$ . It was shown earlier that, at these concentrations of anisotropic proteins with  $\epsilon_{LL} = 0$  protein fields cannot induce large scale aggregation through membrane curvature mediated interaction alone<sup>34</sup> and  $\mathbf{H}_{p\phi}$  interactions are necessary for them to aggregate.

The cluster formation for different values of  $C_0^\parallel$  are shown in Fig. 12(a). The largest protein cluster size  $C_{lp}$  at short time scales are found to be strongly dependent on the induced curvature. For example,  $C_{lp}$  for  $C_0^\parallel = 0.75$ ,  $\epsilon_{LL} = 0$ , exhibits the fastest growth, showing that the proteins can enhance the aggregation through a membrane mediated interaction



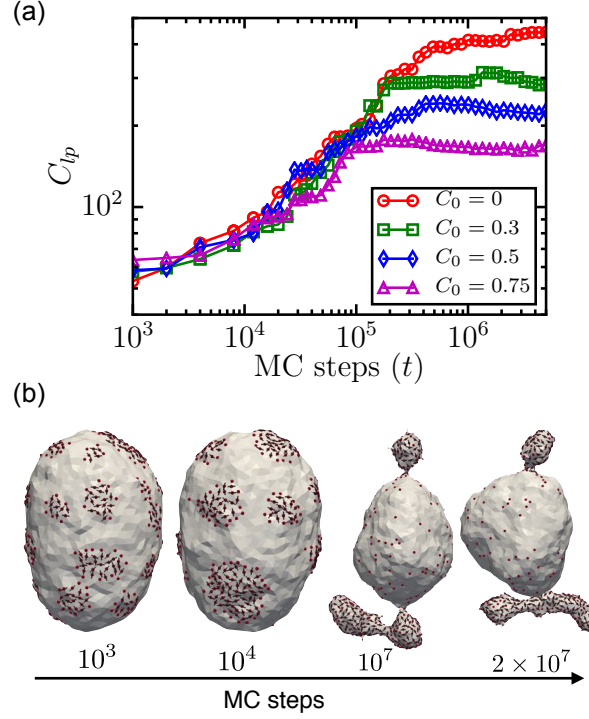


Figure 11. Cluster formation in the presence of isotropic curvature generating proteins as a function of time when  $J_\phi = 0$  and  $J_{p\phi} = 2$ . Panel (a) shows the largest protein cluster size for different values of  $C_0$  and panel (b) the conformations of the vesicle for  $C_0 = 0.3$ .

between the protein fields. The membrane conformations in the presence of curvature active proteins when  $J_{p\phi} = 2$  are shown in Fig. 12(b). Though no explicit orientational interaction between the proteins are included, the proteins in a domain tend to align due to similar induced curvature. At early time the clusters grow faster than those seen for  $C_0^{\parallel} = 0$  (refer Fig. 2(a)). At later times, these domains coalesce resulting in larger clusters until they are big enough to deform the membrane to form tubular structures. Such a large scale aggregation is not observed in the case of proteins that induce isotropic curvature as the domain induced budding occurs at an earlier stage.

#### IV. CONCLUSIONS

We propose a Monte Carlo based multicomponent vesicle model that includes the effect of lipid-lipid, lipid-protein and protein-protein interactions to study (1) the kinetics of protein induced membrane domain formation and (2) the domain induced conformational changes

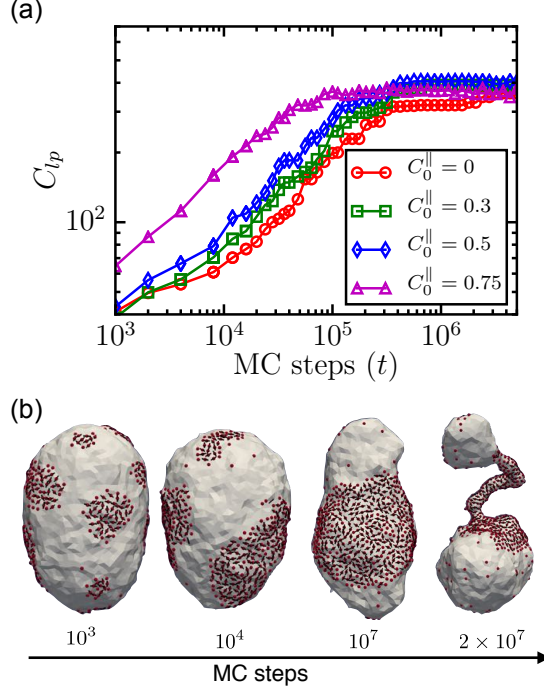


Figure 12. Cluster formation in presence of anisotropic curvature generating proteins as a function of time when  $J_{\phi} = 0$ ,  $J_{p\phi} = 2$ ,  $\epsilon_{LL} = 0$  and  $\kappa_{\parallel} = 5$ . (a)  $C_{lp}$  for different values of  $C_0^{\parallel}$ . (b) The vesicle conformations for induced curvature  $C_0^{\parallel} = 0.75$ .

of the membrane. Our study finds that the lipid-protein interaction induced aggregations to be significantly different from that resulting from lipid-lipid interactions, with the former showing faster cluster formation. The cluster sizes resulting from lipid-protein interactions depend on the protein concentration and on their interaction strength. For small protein fractions ( $p_{\%} < 20$ ) and low lipid-protein interaction strengths ( $J_{p\phi} < 2$ ), the absence of line tension at the domain boundaries lead to fast clustering kinetics. At low co-lipid protein composition ratio and high lipid-protein interactions the effect of line tension is prominent and budding of membrane domains and slowing down of domain growth is observed.

Our simulations explored the effect of lipid-protein interactions on protein clustering and showed that even at small protein concentrations it is possible to get complete protein clustering. We also examined the role of the structural properties of the proteins on the protein aggregation. An explicit protein-protein interaction which prefers parallel alignment of proteins is shown to reduce diffusion of clusters and limits budding of domains. The clustering of curvature active proteins is shown to have significant dependence on the anisotropy of the

induced curvature, with stronger anisotropy suppressing budding and favoring larger cluster formation.

## Appendix A: Scaling of domains

Scaling assumption implies that the distance between domains  $d$  should scale the same way as the size of the domain size itself. For circular domains of radius  $R$ , this would imply that  $d \propto R$ . If the domain coalescence takes place through diffusion of domains then the coalescence time  $t_c$  scales as  $d^2 \propto Dt_c$ , where  $D$  is the diffusion coefficient. Rouse dynamics implies that  $D \propto 1/R^2$ , i.e.,  $D$  is inversely proportional to the number of vertices in the domain. Thus  $d^2 \propto t_c/R^2$  which leads to  $R^4 \propto t_c$ . Therefore  $R \propto t^{1/4}$  and the size of the domains scales as  $t^{1/2}$ .

## REFERENCES

- <sup>1</sup>K. Simons and D. Toomre, “Lipid rafts and signal transduction,” [Nat Rev Mol Cell Biol](#) **1**, 31 (2000).
- <sup>2</sup>R. Sarasij, S. Mayor, and M. Rao, “Chirality-induced budding: A raft-mediated mechanism for endocytosis and morphology of caveolae?” [Biophys. J.](#) **92**, 3140–3158 (2007).
- <sup>3</sup>D. Goswami, K. Gowrishankar, S. Bilgrami, S. Ghosh, R. Raghupathy, R. Chadda, V. Rand, M. Rao, and S. Mayor, “Nanoclusters of gpi-anchored proteins are formed by cortical actin-driven activity,” [Cell](#) **135**, 1085–1097 (2008).
- <sup>4</sup>K. Gowrishankar, S. Ghosh, S. Saha, C. Rumamol, S. Mayor, and M. Rao, “Active remodeling of cortical actin regulates spatiotemporal organization of cell surface molecules,” [Cell](#) **149**, 1353–1367 (2012).
- <sup>5</sup>R. Raghupathy, A. Anilkumar, A. Polley, P. Singh, M. Yadav, C. Johnson, S. Suryawanshi, V. Saikam, S. Sawant, A. Panda, Z. Guo, R. Vishwakarma, M. Rao, and S. Mayor, “Transbilayer lipid interactions mediate nanoclustering of lipid-anchored proteins,” [Cell](#) **161**, 581–594 (2015).
- <sup>6</sup>K. Simons and E. Ilkon, “Functional rafts in cell membranes,” [Nature](#) **387**, 569–572 (1997).
- <sup>7</sup>K. Simons and W. L. Vaz, “Model systems, lipid rafts, and cell membranes,” [Annual Review of Biophysics and Biomolecular Structure](#) **33**, 269–295 (2004).

- <sup>8</sup>M. Mercker and A. Marciniak-Czochra, “Bud-neck scaffolding as a possible driving force in esrt-induced membrane budding,” [Biophys. J.](#) **108**, 833–843 (2015).
- <sup>9</sup>C. Barlowe, L. Orci, T. Yeung, M. Hosobuchi, S. Hamamoto, N. Salama, M. F. Rexach, M. Ravazzola, M. Amherdt, and R. Schekman, “Copii: A membrane coat formed by sec proteins that drive vesicle budding from the endoplasmic reticulum,” [Cell](#) **77**, 895–907 (1994).
- <sup>10</sup>B. Antonny, “Membrane deformation by protein coats,” [Curr. Opin. Cell Biol.](#) **18**, 386–394 (2006).
- <sup>11</sup>J. Poveda, A. Fernandez, J. Encinar, and J. Gonzalez-Ros, “Protein-promoted membrane domains,” [Biochim. Biophys. Acta](#) **1778**, 1583–1590 (2008).
- <sup>12</sup>R. M. Epand, “Proteins and cholesterol-rich domains,” [Biochim. Biophys. Acta](#) **1778**, 1576–1582 (2008).
- <sup>13</sup>Q.-Y. Wu and Q. Liang, “Interplay between curvature and lateral organization of lipids and peptides/proteins in model membranes,” [Langmuir](#) **30**, 1116–1122 (2014).
- <sup>14</sup>S. Mayor and H. Riezman, “Sorting gpi-anchored proteins,” [Nat. Rev. Mol. Cell Biol.](#) **5**, 110–120 (2004).
- <sup>15</sup>R. G. W. Anderson and K. Jacobson, “A role for lipid shells in targeting proteins to caveolae, rafts, and other lipid domains,” [Science](#) **296**, 1821–1825 (2002).
- <sup>16</sup>M. G. J. Ford, I. G. Mills, B. J. Peter, Y. Vallis, G. J. K. Praefcke, P. R. Evans, and H. T. McMahon, “Curvature of clathrin-coated pits driven by epsin,” [Nature](#) **419**, 361–366 (2002).
- <sup>17</sup>P. Drucker, M. Pejic, H.-J. Galla, and V. Gerke, “Lipid segregation and membrane budding induced by the peripheral membrane binding protein annexin a2,” [Journal of Biological Chemistry](#) **288**, 24764–24776 (2013).
- <sup>18</sup>R. Oliva, P. D. Vecchio, M. I. Stellato, A. M. D’Ursi, G. D’Errico, L. Paduano, and L. Petraccone, “A thermodynamic signature of lipid segregation in biomembranes induced by a short peptide derived from glycoprotein gp36 of feline immunodeficiency virus,” [Biochimica et Biophysica Acta \(BBA\) - Biomembranes](#) **1848**, 510 – 517 (2015).
- <sup>19</sup>G. van Meer, D. R. Voelker, and G. W. Feigenson, “Membrane lipids: where they are and how they behave,” [Nature](#) **9**, 112–124 (2008).
- <sup>20</sup>G. van Meer and A. I. P. M. de Kroon, “Lipid map of the mammalian cell,” [Journal of Cell Science](#) **124**, 5–8 (2011).

- <sup>21</sup>S. McLaughlin and D. Murray, “Plasma membrane phosphoinositide organization by protein electrostatics,” *Nature* **438**, 605–611 (2005).
- <sup>22</sup>A. Frost, V. M. Unger, and P. D. Camilli, “The bar domain superfamily: Membrane-molding macromolecules,” *Cell* **137**, 191–196 (2009).
- <sup>23</sup>G. van den Bogaart, K. Meyenberg, H. J. Risselada, H. Amin, K. I. Willig, B. E. Hubrich, M. Dier, S. W. Hell, H. Grubmüller, U. Diederichsen, and R. Jahn, “Membrane protein sequestering by ionic protein-lipid interactions,” *Nature* **479**, 552–555 (2011).
- <sup>24</sup>P. B. Sunil Kumar and M. Rao, “Shape Instabilities in the Dynamics of a Two-Component Fluid Membrane,” *Phys. Rev. Lett.* **80**, 2489–2492 (1998).
- <sup>25</sup>P. B. Sunil Kumar, G. Gompper, and R. Lipowsky, “Budding dynamics of multicomponent membranes,” *Phys. Rev. Lett.* **86**, 3911–3914 (2001).
- <sup>26</sup>M. Laradji and P. Sunil Kumar, “Dynamics of Domain Growth in Self-Assembled Fluid Vesicles,” *Phys. Rev. Lett.* **93**, 198105 (2004).
- <sup>27</sup>M. Laradji and P. B. Sunil Kumar, “Domain growth, budding, and fission in phase-separating self-assembled fluid bilayers,” *J. Chem. Phys.* **123**, 224902 (2005), [10.1063/1.2102894](https://doi.org/10.1063/1.2102894).
- <sup>28</sup>L. Li, X. Liang, M. Lin, F. Qiu, , and Y. Yang, “Budding dynamics of multicomponent tubular vesicles,” *Journal of the American Chemical Society* **127**, 17996–17997 (2005).
- <sup>29</sup>S. Ramachandran, M. Laradji, and P. B. S. Kumar, “Lateral organization of lipids in multi-component liposomes,” *J. Phys. Soc. Jpn.* **78**, 041006 (2009).
- <sup>30</sup>N. Ramakrishnan, P. B. S. Kumar, and J. H. Ipsen, “Monte carlo simulations of fluid vesicles with in-plane orientational ordering,” *Phys. Rev. E* **81**, 041922 (2010).
- <sup>31</sup>B. J. Peter, H. M. Kent, I. G. Mills, Y. Vallis, P. J. G. Butler, P. R. Evans, and H. T. McMahon, “Bar domains as sensors of membrane curvature: The amphiphysin bar structure,” *Science* **303**, 495–499 (2004).
- <sup>32</sup>P. A. Lebwohl and G. Lasher, “Nematic-liquid-crystal order—a monte carlo calculation,” *Phys. Rev. A* **6**, 426–429 (1972).
- <sup>33</sup>J. R. Frank and M. Kardar, “Defects in nematic membranes can buckle into pseudo-spheres,” *Phys. Rev. E* **77**, 041705 (2008).
- <sup>34</sup>N. Ramakrishnan, P. B. S. Kumar, and J. H. Ipsen, “Membrane-mediated aggregation of curvature-inducing nematogens and membrane tubulation,” *Biophys. J.* **104**, 1018–1028 (2013).

- <sup>35</sup>Y. Han, Y. Shokef, A. M. Alsayed, P. Yunker, T. C. Lubensky, and A. G. Yodh, “Geometric frustration in buckled colloidal monolayers,” [Nature](#) **456**, 898–903 (2008).
- <sup>36</sup>E. J. Ungewickell and L. Hinrichsen, “Endocytosis: clathrin-mediated membrane budding,” [Curr. Opin. Cell Biol.](#) **19**, 417–425 (2007).
- <sup>37</sup>R. M. Epand, B. G. Sayer, and R. F. Epand, “Caveolin scaffolding region and cholesterol-rich domains in membranes,” [Journal of Molecular Biology](#) **345**, 339 – 350 (2005).
- <sup>38</sup>P. K. Mattila, A. Pykäläinen, J. Saarikangas, V. O. Paavilainen, H. Vihinen, E. Jokitalo, and P. Lappalainen, “Missing-in-metastasis and irsp53 deform pi(4,5)p2-rich membranes by an inverse bar domain like mechanism,” [The Journal of Cell Biology](#) **176**, 953–964 (2007).
- <sup>39</sup>Y. Zhao, J. Liu, C. Yang, B. Capraro, T. Baumgart, R. Bradley, N. Ramakrishnan, X. Xu, R. Radhakrishnan, T. Svitkina, and W. Guo, “Exo70 generates membrane curvature for morphogenesis and cell migration,” [Dev. Cell](#) **26**, 266–278 (2013).